Vol. 19, No. 3 (2020) 1413-1423
Revista Mexicana de Ingeniería Química

Effect of the adsorbent dose in Pb(II) removal by using sugar cane bagasse: Kinetics and isotherms

Efecto de la dosis de adsorbente en la remoción de Pb(II) usando bagazo de caña de azúcar: Cinética e isotermas

C. Tejada-Tovar[1], H. Bonilla-Mancilla[2], J. del Pino-Moreyra[3], A. Villabona-Ortíz[1] and R. Ortega-Toro[4]*

[1] *Universidad de Cartagena, Chemical Engineering Department, Process Design and Biomass Utilization Research Group (IDAB), Avenida del Consulado Calle 30 No. 48 - 152, Cartagena de Indias D.T. y C., Colombia 130015.*
[2] *Universidad Nacional del Centro del Perú, Faculty of Forestry and Environmental Sciences. Mariscal Castilla 3909, Huancayo, Perú, 12006.*
[3] *Universidad Nacional del Centro del Perú, Nursery Faculty. Mariscal Castilla 3909, Huancayo, Perú, 12006.*
[4] *Universidad de Cartagena, Food Engineering Department, Food Packaging and Shelf Life Research Group (FP&SL) y Grupo de Investigación Ingeniería de Fluidos Complejos y Reología de Alimentos (IFCRA), Avenida del Consulado Calle 30 No. 48 - 152, Cartagena de Indias D.T. y C., Colombia 130015.*

Received: December 17, 2019; Accepted: February 17, 2020

Abstract

The objective of this work was to evaluate the effect of the adsorbent dose on the removal of lead (II) present in a synthetic solution using sugarcane bagasse (*Saccharum officinarum*). The biomaterial was characterized before and after removal by FTIR analysis which reported the presence of hydroxyl, carboxyl and carbonyl functional groups; and SEM analysis showing a porous surface in the form of fibrous cylinders typical of lignocellulosic materials, evidencing that Pb (II) ions are captured on the surface of the adsorbent. It was determined that the best dose of adsorbent was 0.10g obtaining 99.68% removal. The results of the kinetics were adjusted by the first order Pseudo model; and the isothermal adsorption that described the process was Langmuir, determining that the process occurs by physic-sorption and monolayer. It is concluded that the residual cane bagasse is efficient for the preparation of adsorbent and is recommended for the removal of the metal ion under study.

Keywords: sugar cane residual bagasse, physical morphology, Lead (II), interaction, kinetics.

Resumen

El objetivo del presente trabajo fue evaluar el efecto de la dosis de adsorbente en la remoción de plomo (II) presente en solución sintética usando bagazo de caña de azúcar (*Saccharum officinarum*). El biomaterial fue caracterizado antes y después de la remoción por análisis FTIR el cual reportó la presencia de grupos funcionales hidroxilo, carboxilo y carbonilo; y análisis SEM mostrando una superficie porosa en forma de cilindros fibrosos típica de materiales lignocelulósicos, evidenciando que los iones Pb (II) se adsorbieron en la superficie del adsorbente. Se determinó como la mejor dosis de adsorbente 0,10 g obteniendo 99,68% de remoción. Los resultados de la cinética fueron ajustados por el modelo de Pseudo primer orden; y la isoterma adsorción que describió el proceso fue Langmuir determinando que el proceso se da por fisisorción y en monocapa. Se concluye que el bagazo de caña residual es eficiente para la preparación de adsorbente y se recomienda para la eliminación del ion metálico en estudio.

Palabras clave: bagazo de caña residual, morfología física, Plomo (II), interacción, cinética.

1 Introduction

The discharge of effluents containing heavy metals to surface water bodies causes environmental problems, not only because they are toxic, but also resistant to degradation, bio accumulative in biota at different trophic levels, and thus contaminate food chains by bio-magnifying through these (Marimón-Bolívar *et al*., 2018; Ávila-Manzanares *et al*., 2019; Villabona-Ortíz *et al*., 2020). Lead enters the water bodies due to a variety of industrial wastewater such as paper and pulp, mining, electroplating, lead smelting and metallurgical finishing, dyeing, storage batteries, textile and automotive industries (Basu *et al*., 2017).

* *Corresponding author. E-mail*: rortegap1@unicartagena.edu.co
https://doi.org/10.24275/rmiq/IA1101
ISSN 1665-2738, issn-e: 2395-8472

The presence of Pb (II) in plants can cause leaf necrosis, developmental delay and root growth (Tejada-Tovar *et al*., 2015a). Lead ions bioaccumulate in the bones with a half-life of 20 years, and can damage the kidneys, liver, brain and nervous system function, basic cellular processes, the reproductive system, and due to their enzyme inhibitory effects, it is a probable carcinogen (Chu *et al*., 2019; Morosanu *et al*., 2017). Pb (II) ions have a high affinity for the thiol (SH), oxo (= O) and phosphate (PO_4^{-3}) groups found in some enzymes, and also ligands and biomolecules of the organism and affect the permeability of the organ membrane and haemoglobin synthesis (Morosanu *et al*., 2017).

Lead is on the list of priority pollutants of the US Environmental Protection Agency (US-EPA) (US-EPA, 2014); and the World Health Organization (WHO), established as a maximum permitted concentration for Pb (II) in water the limit value of 0.01 mg/L. However, concentrations of up to 0.735 ppm are currently reported in rivers (Tejada-Tovar *et al*., 2018). Thus, different physicochemical treatments have been applied to decrease the concentration of lead in effluents and involve chemical precipitation, reduction, electrochemical methods, adsorption, ion exchange, adsorption, flotation, reverse osmosis, coagulation, ultrafiltration, among others (Kariuki *et al*., 2017). The most common drawbacks of adsorption techniques are the high price of adsorbents, such as activated carbon (Alhogbi, 2017), making low cost bio adsorbents in adsorption processes, an alternative to conventional methods; and includes the use of dead biomass (agricultural by-products such as fibre, peat and wool) as well as algae, bacteria, fungi, and among other living biomass (Lawal *et al*., 2017). The bio adsorption, takes advantage of the availability of waste, its low cost, regeneration, high efficiency, and the capacity of union of the active centres of the biomass with the heavy metals thanks to which they are composed of lignin and cellulose, thus including polar functional groups of lignin as: alcohols, aldehydes, ketones, carboxylic groups, phenolics and ether (Obike *et al*., 2018).

In the removal of lead in solution, various bio-absorbents such as coffee waste (Alhogbi, 2017), corn silk (Karimi *et al*., 2018), peanut peel, plantain (Vilardi *et al*., 2018), walnut (Çelebi and Gök, 2017), orange (Giza, 2017), cucumber (Basu *et al*., 2017), have been used among others (Sahmoune, 2019; Jena and Sahoo, 2017); determining the effect of parameters such as pH, adsorbent dose, contact time, temperature and initial concentration, in the removal of the metal ion, finding that biomaterials of plant origin have a good performance in the removal of Lead (II) due to its contact area, lignocellulosic nature, high adsorption capacity and rapid kinetics (Karimi *et al*., 2018; Basu *et al*., 2017). The processing of agricultural products often produces large proportions of by-products. Sugarcane (*Saccharum officinarum*) is a plant species belonging to the family of the poaceae and widely cultivated in tropical areas of the world, and is mainly composed of lignin (18%), cellulose (45%), hemicellulose (28%) and few proteins (6%) ; so in its structure it would have the presence of carboxylic acids, hydroxyls, esters, amines, phosphates and alkanes, which would make it a good precursor for heavy metal adsorbent (Ibraheem *et al*., 2018). Cane bagasse is a solid waste generated in large volumes from the exploitation of sugarcane cultivation. In Peru about 10 million tons of sugarcane are produced, of which 30% is bagasse at the end of the sugar extraction process (Pollack-Velásquez *et al*., 2018). In this context, the effect of the dose of adsorbent on the ability to remove Lead (II) present in aqueous solution on sugarcane bagasse (*Saccharum officinarum*) was studied in this investigation.

2 Materials and methods

2.1 Materials

The sugarcane bagasse was collected from the province of Huancayo-Peru. Silver Nitrate ($Pb(NO_3)_2$) 99.0% LOBA-Chemie brand analytical grade was used. Sodium hydroxide (NaOH) and Nitric acid (HNO_3) were used to adjust the pH

2.2 Experimental design

A completely randomized DCA experiment design was used evaluating three levels of adsorbent dose variation: 0.05; 0.075 and 0.1 g. All experiments were performed in triplicate

2.3 Biomass preparation and characterization

The biomass was washed to remove impurities and soluble compounds, then dried at 55 ° C for 72 hours, until a constant mass was reached; subsequently, it was ground and sieved using a 1 mm sieve. Sugarcane bagasse was characterized by FTIR analysis in a range of 4000-400 cm^{-1} using a Perkin Elmer Frontier

Dual-Range spectrometer, to establish the presence of functional groups present in the material that actively participate in the process of metal ion removal. SEM analysis was also performed for the morphological characterization of biomass, using a Hitachi SU8230 SEM scanning electron microscope with 100 and 500 μm magnifications.

2.4 Adsorption essays

Adsorption tests were performed by placing 50 mL of solution at 50 ppm in contact with the adsorbent of 2 g/L at room temperature, with a stirring of 180 rpm, pH 5 for 40 min. Removal efficiency (%) was determined according to equation 1 (Villabona-Ortíz *et al*., 2020).

$$Removal\ percentage\ (\%) = \frac{C_i - C_f}{C_i} * 100 \quad (1)$$

where C_i represents the initial concentration and C_f the final concentration in ppm.

The absorption capacity was determined according to equation 2.

$$q_e = \frac{(C_0 - C_e)V}{M} \quad (2)$$

where C_0 and C_e are initial and equilibrium concentrations in ppm respectively; V stands for the solution volume in L, M the adsorbent mass in g and q_e is the adsorbate concentration in equilibrium in mg/g.

The concentration of residual Pb (II) in solution was determined by atomic absorption using an AGILENT AA 280FS Atomic Absorption Spectrophotometer.

2.5 Bio adsorption kinetics

The adsorption kinetics provides information on the time in which the adsorbent material manages to retain the maximum amount of solute (the adsorption equilibrium time) (Adamu *et al*., 2018). 0.1 g of biomass was contacted with 50 mL of solution at 150 ppm of Pb (II) at pH 5, 150 rpm of stirring; Aliquots were taken every certain period of time (5, 10, 15, 20, 30, 40, 50, 60, 80, 100 and 120 min). The concentration of Pb (II) remaining in the solution was determined by atomic absorption at 217 nm. The data obtained were adjusted to the kinetic models described in Table 1.

2.6 Adsorption isotherms

The adsorption isotherms were performed with the aim of describing the balance of the Lead split between the solid and liquid phases. To accomplish the isotherms, 0.1 g of bio adsorbent was placed in contact with 50 mL of contaminant solution at different concentrations (25, 50, 75, 100 and 125 ppm), pH 5 and 180 rpm for 25 min (Ma *et al*., 2018). The isothermal data obtained were adjusted to the Langmuir and Freundlich models, described in Table 2.

Table 1. Kinetic adsorption models.

Model	Equation	Parameters
Lagergren or Pseudo-first order	$q_t = q_e\,(1 - e^{-k_1 t})$	q_e (mg/g): Adsorption capacity in equilibrium q_t (mg/g): Adsorption capacity in a t time k_1 (min^{-1}): Lagergren constant
Pseudo-Second order	$q_t = \frac{t}{\frac{1}{k_2 q_e^2} + \frac{t}{q_e}}$	k_1 (g^{-1} min^{-1}): Pseudo-second constant
Elovich	$q_t = \frac{1}{\beta}\ln(\alpha\beta) + \frac{1}{\beta}\ln(t)$	α (mg g^{-1} min^{-1}): adsorption velocity β (g/mg): Elovich constant related with the scope of the surface coverage and activation energy in the chemisorption

Source: Villabona-Ortíz et al., 2020; Vilardi et al., 2018; Vizcaíno-Mendoza et al., 2017.

Table 2. Adsorption isotherms models.

Model	Equation	Parameter
Langmuir	$\frac{1}{q} = \frac{1}{q_{max}} + \frac{1}{b * q_{max} * C_e}$	q_{max} (mg/g): máximum quantity of Pb (II) captured in the adsorbent. b: Langmuir constant related with adsorbent affinity to the contaminant C_e: Adsorbate concentration in equilibrium
Freundlich	$\log q = \frac{1}{n}\log C_e + \log K$	n: Adsorption intensity according to its heterogeneity. K: Freundlinch constant related with adsorption capacity.

Fuente: Guiza, 2017; Tejada-Tovar et al., 2015b; 2016.

2.7 Statistical analysis

The experimental data were evaluated by the statistical software MINITAB 18. A completely randomized DCA design was developed, choosing as independent variable: amount of biomass and as dependent variable: removal capacity (% removal) and to determine significant differences between the means used a unidirectional ANOVA (analysis of variance) followed by the Tukey's means test. with a P-value <0.05.

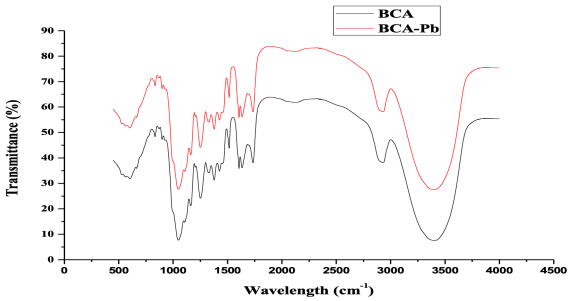

Fig. 1. FTIR spectrum of sugarcane bagasse (BCA) before and after the adsorption process of Pb (II).

3 Results and discussion

3.1 FTIR analysis

According to the spectrum shown in Figure 1, the sugarcane bagasse biomass has a heterogeneous and multiple surface reflected in the absorbance spectrum with multiple peaks. The vibration of the 3438.8 cm^{-1}, 3448.13 and 3429.4 cm^{-1} peaks confirms the streaching of hydroxyl and amines, and presence of alcohol and ether functional groups, respectively, present in the lignin and cellulose structure (Adamu *et al*., 2018). The 1595.0 cm^{-1} peak corresponds to the C = C carboxylic group, known as aromatic rings, and the 1630 cm^{-1} band belongs to the stretching of the amide (C = O) characteristic of the peptone (Marimón-Bolívar *et al*., 2018). The band 1141.8 cm^{-1} represents the phenolic groups (C−O and O−H) (Basu *et al*., 2017; Lawal *et al*., 2017). The presence of these functional groups in the structure of cane bagasse is attributed to the presence of cellulose, hemicellulose, pectin and lignin, typical of lignocellulosic materials, and are branched or linear long chain polymers.

They are present in cell walls of plants and are primarily responsible for the adsorption of metal ions (Cruz *et al*., 2018; Tejada-Tovar *et al*., 2015b). After lead adsorption many changes are shown in the FTIR spectrum; the peak between 3200-3600 cm^{-1} has been relocated which implies the widening of the O−H and N−H groups at the metal junction. The vibrations at 2952.61 cm^{-1} and 2880.54 cm^{-1} confirm the participation of carboxylic acid and alkanes, in the uptake of the ion present in the solution. The peak was reallocated to 1435.98 cm^{-1} to 1437.58 cm^{-1} after adsorption. The displacement of the wave number located at 1323.87 cm^{-1} indicates the participation of the carboxyl and hydroxyl group in the process of metallic union with the active centres of the biomass. The association of P = O and C = S in the adsorption process is evident by the transfer of the peak at 1240.59 cm^{-1}. Stretch vibrations C = S and S = O have also changed from 1165.32 cm^{-1} to 1162.12 cm^{-1}. Which suggests an active participation of the functional groups present in the cane bagasse in the process of metallic uptake, through chemical bonds (Tejada-Tovar, 2019).

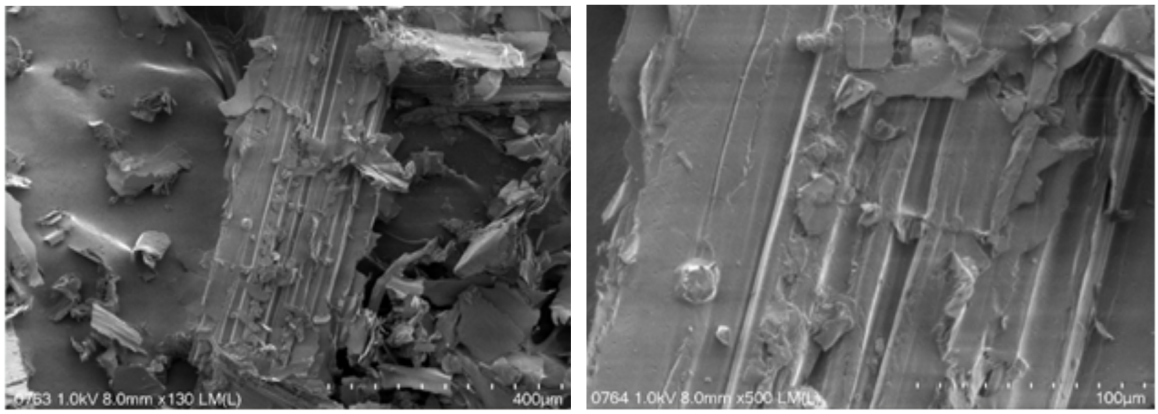

Fig 2. SEM 400 um (a) microphotographs; and 100 um (b) before adsorption.

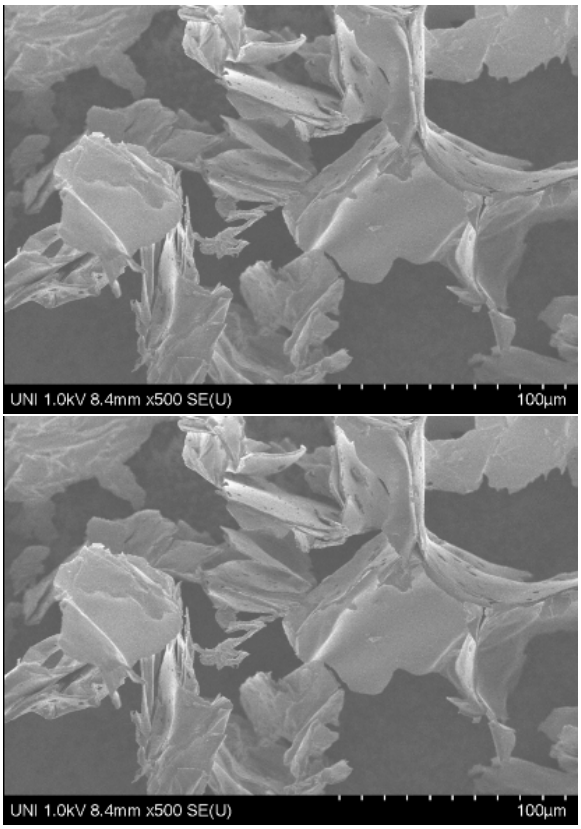

Fig. 3. SEM micrographs of the BCA after the adsorption process of Pb (II).

3.2 Electron microscopy (SEM)

The SEM analysis of Figure 3 shows an irregular and porous structure of the sugarcane bagasse; as well as a heterogeneous structure with a laminated appearance, allowing a better heterogeneous biosorption due to the large adsorption surface (Canlas *et al*., 2019). A defined appearance was observed in the form of fibrous cylinders with porosity that is typical of lignocellulosic materials (Jena & Sahoo, 2017).

Figure 3 shows the SEM micrographs for biomass after batch adsorption experiments. It was found that Pb (II) ions were adsorbed on the surface of the SCB following an electrostatic attraction mechanism (Medellín-Castillo *et al*., 2017; Marimón-Bolívar *et al*., 2019). Likewise, it is observed that there are no agglomerations of the ion on the surface of the adsorbent, so it is assumed that there was no formation of micro precipitated complexes or chelates on the sample (Medellín-Castillo *et al*., 2017; Torres-Santillán *et al*., 2018).

The spectrogram and elementary composition of the SCB obtained by EDS is shown in Figure 4. The presence of heavy metal ion precipitation on the adsorption surface was identified with a mass weight percentage of 0.93% for the adsorbent under study.

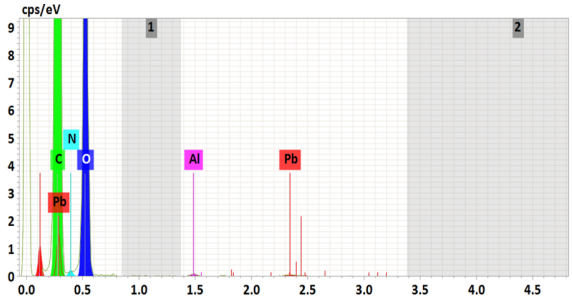

Fig. 4. EDS spectrum of the SCB after adsorption of Pb (II).

Such results are attributed to the formation of bonds between active sites of lignocellulosic material (Figure 1) and ions. In addition, it was found that C and O are the most abundant elements with 54.42% and 45.52%, respectively; what is due to the presence of active sites without saturation when taking the sample. The above, shows a good indicator regarding the capacity of elimination of bio-adsorbents and reuse of the material (Tejada-Tovar *et al*., 2019).

3.3 Effect of the adsorbent

The cations in the solution can be adsorbed on the surface of the material due to electrostatic forces, forming complexes and chelates. Once these compounds are formed, they migrate more easily through the adsorbent (Narkar & Bera, 2017). Thus, Table 3 shows the data on the removal of Pb (II), the assessment had three repetitions and was evaluated by completely randomized design (DCA), using the software MINTAB 18, which showed a p-value 0.05, existing a significant difference between the three adsorbent weights (0.05; 0.075 and 0.1 g); establishing that the increase in the adsorbent dose has a positive linear impact on the adsorption percentage, reaching adsorption efficiencies greater than 99% and an adsorption capacity on the surface of the cane bagasse of 12.46 mg/g.

In Table 3 it is observed that as the adsorbent dose increased from 0.05 to 0.1 g, the adsorption capacity decreased from 24.04 to 12.46 mg/g; This is explained because the surface area and availability of active sites of the biomaterial is proportional to the amount of adsorbent in contact with the contaminated solution. However, with a high amount of adsorbent the available ions of Pb (II) are insufficient to cover all adsorption sites, as well as the agglomeration of active sites, which results in low adsorption of the metal (Tatah *et al*., 2017).

Table 4 shows values of Pb (II) removal reported by different authors, regarding the capacities and percentages of removal.

3.4 Adsorption isotherms

The adsorption isotherm represents the affinity of the adsorbent with the adsorbate (Leizou *et al*., 2018). The adjustment of the experimental adsorption equilibrium data of the Pb (II) ions is shown in Figure 3. The parameters of the isothermal models were evaluated by non-linear regression and are shown in Table 4.

Table 3. Percentage of lead (II) ions removal in synthetic solution.

Essay	Adsorbent dose (g)	C_f (ppm)	q_e (mg/g)	Removal percentage %
1	0.050	0.96	24.04	96.16
2	0.050	0.90	24.10	96.4
3	0.050	0.92	24.08	96.32
4	0.075	0.42	16.39	98.32
5	0.075	0.37	16.42	98.52
6	0.075	0.41	16.39	98.36
7	0.100	0.06	12.47	99.76
8	0.100	0.10	12.45	99.6
9	0.100	0.08	12.46	99.68

Table 4. Comparison between adsorption capacities and percentages.

Biomass	**q_e (mg/g)**	**Removal %**	**Activation**	**Source**
Orange peel	495.98	99.20%	$CaCl_2$	Tejada-Tovar et al., 2016
Plantain peel	3.063	91.682	WA	Leizou et al., 2018
Orange peel	9.39	99.50	$CaCl_2$	Cardona: 2013
Almond-tree peel	1.9912	99.56	AC	Canlas et al., 2019
Corn cob	2687.74	85.00	WA	Tejada-Tovar et al., 2016
Sugar cane bagasse	86.96	80.00	AC	Adamu et al., 2018
Cucumber peel	133.6	94.50	A. formic	Basu; 2017
Sugar cane bagasse	12.46	99.68	WA	Present study

WA: without activation AC: activated charcoal

Table 5. Parameters of the adsorption isotherm of Pb (II).

Model	Parameters	
Langmuir	q_{max} (mg/g)	37.883
	b	1.604
	R^2	0.974
	SS	35.993
Freundlich	K_f	21.372
	1/n	0.156
	n	6.410
	R^2	0.964
	SS	40.853

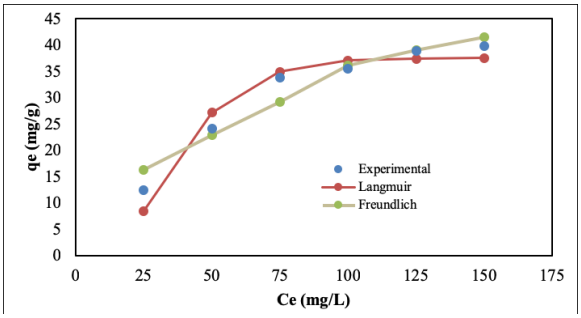

Fig. 5. Fit of the models to the adsorption isotherms of Pb(II).

From Figure 3 and the values of the parameters reported in Table 4, it is established that the model that best adjusts the lead adsorption balance is that of Langmuir, which suggests that the surface of the adsorbent is uniform, all sites of adsorption are equivalent, adsorbed molecules do not interact, adsorption occurs through the same mechanism and that in maximum adsorption only a monolayer is formed where adsorbate molecules are not deposited on others already adsorbed (Basu *et al*., 2017; Mohammad-Rezaei and Jaymand, 2019). The above can be attributed to the homogeneous distribution of the binding sites in the adsorbents (Tatah *et al*., 2017). The affinity of the metal for the adsorbent surface in terms of parameter b was low, which implies a low surface energy in the process and, consequently, a weak bond between the metal ions and the adsorbent (indicating a physic-sorption mechanism) that marks the recovery of metal ions through easy desorption, which is an important criterion for selecting an adsorbent (Verma and Sarkar, 2018; Zhou *et al*., 2017). Based on the Langmuir isotherm, the maximum adsorption capacity (qmax) of Pb (II) was estimated at 37.883 mg / g, which is close to the results obtained using coffee residues (37.037 mg/g) (Alhogbi, 2017), and significantly higher than those obtained with tea residues (21.395 mg/g) (Nikolic *et al*., 2019).

The Freundlich parameter n, associated with the adsorption intensity shows the types of process. The value of n> 1 indicates that the adsorption is physical in nature, the process is chemical in nature if the values of n are <1, also that the bonds formed between the ion and adsorbent are strong, and that the process adsorption is favourable (Nikolic *et al*., 2019). Thus, from the values obtained from n it can be inferred that the accumulation of the contaminant on the solid surface is of a physical nature (Singh *et al*., 2018; Ray *et al*., 2018).

3.5 *Adsorption kinetics*

The kinetic study is carried out in order to know the behaviour of the adsorption process over time. Figure 4 shows the adjustment of the data obtained in the adsorption tests and the adjustment to the kinetic models of Pseudo-first order, Pseudo-second order and Elovich, observing rapid adsorption during the first minutes and stabilization after 40 min.

The fit parameters of the models used were found by non-linear adjustment and are shown in Table 3. It was found that the pseudo-first order model best describes the adsorption kinetics of Pb (II), according to the coefficient of correlation obtained and the adjustment presented in Figure 4. The adjustment to this model establishes that the process is controlled by physic-sorption and describes the rate of chelation of pectin (Chu *et al*., 2019; Villegas-García *et al*., 2011).

Table 6. Calculated parameters of adsorption kinetics.

Model	Parameter	Value
Pseudo-first order	q_{max} (mg/g)	19,9915
	K_1 (min^{-1})	0,2086
	R^2	0,9993
	SS	3.6521
Pseudo second- order	q_e (mg/g)	21,1032
	K_2 (g^{-1} min^{-1})	0,0191
	R^2	0,9875
	SS	0.8315
Elovich	B	0.5442
	A	1749.37
	R^2	0.9023
	SS	0.0071

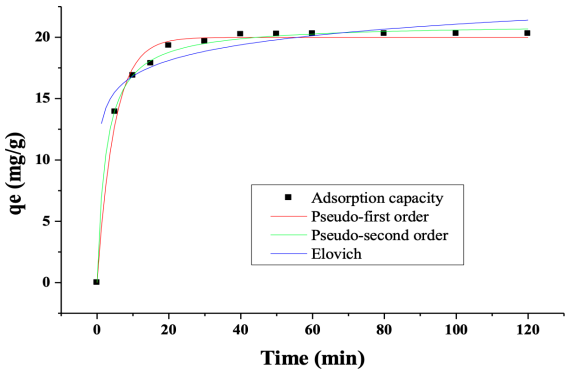

Fig. 6. Fit to the kinetic models.

However, the pseudo-second order model also presented a good fit, which states that the metal ion can be adsorbed by two active biomass sites. From the value of the constant k_2 it is shown that the initial sorption rate for Pb (II) is low, thus, also achieving a low adsorption efficiency. Likewise, the Elovich model also presented a good adjustment according to the sum of errors of 0.0071, the correlation coefficient of 0.9023 and the parameter α of 1749.37 mg/g min, therefore, it can be said that the adsorption of Pb (II) takes place inside the pores of the particles of bio adsorbent materials considering the heterogeneity of the active sites of the adsorbent found in the FTIR spectrum of Figure 1, so they exhibit different activation energies throughout the adsorption process (Doke and Khan, 2017; Celebi *et al*., 2017).

Conclusions

From the FTIR analysis, the presence of functional groups characteristic of lignocellulosic materials was established, which are responsible for the capture of metal ions. From the adsorption tests it was found that the adsorbent dose proportionally influences the adsorption efficiency and a high affinity of the bio adsorbent for the metal ion was demonstrated reaching a removal rate of 99.68% and an adsorption capacity of 12.46 mg/g. The experimental data were adjusted to the kinetic model of Pseudo - first order and that of Langmuir isotherm, and a maximum adsorption capacity 37.883 mg/g determining that the process is controlled by physic-sorption and is given in monolayers. It is concluded that residual cane bagasse is efficient for the elimination of Lead (II) present in aqueous solutions.

Acknowledgements

The authors thank the Universidad Nacional del Centro del Perú and to the Universidad de Cartagena (Colombia) for the support in the development of this work regarding laboratory, software use and time for their researchers.

Nomenclature

q_e:	adsorption capacity in equilibrium
q_t:	adsorption capacity in a t time
k_1:	Pseudo-first order constant
k_2:	Pseudo-second constant
T:	Time
α:	adsorption velocity
β:	constant related with the scope of the surface coverage and activation energy in chemisorption
qmax:	maximum amount of adsorption in the adsorbent
SCB:	Sugarcane bagasse

References

Adamu, A. D., Adie, D. B., Okuofu, C. A., & Giwa, A. (2018). Application of activated carbon prepared from sugarcane bagasse for lead removal from wastewater. *ATBU Journal of Science, Technology and Education 6*, 126-140.

Ávila-Manzanares, J.E., Santacruz, H., & Machi, L. (2019). Pyrene bichromophores supported on polymer beads: a new library of fluorescent materials for sensing heavy metals in water. *Revista Mexicana de Ingeniería Química 18*, 513-529. https://doi.org/10.24275/uam/izt/dcbi/revmexingquim/2019v18n2/Avila

Basu, M., Guha, A. K., & Ray, L. (2017). Adsorption of lead on cucumber peel. *Journal of Cleaner Production 151*, 603-615. https://doi.org/10.1016/j.jclepro.2017.03.028

Canlas, J. J., Go, J. C., Mendoza, A. C., & Dimaano, M. N. (2019). Talisay (Terminalia catappa) seed husk biochar for adsorption of lead (II) ions in artificially contaminated soil. In MATEC Web of Conferences 268, 04011. *EDP Sciences*. https://doi.org/10.1051/matecconf/201926804011

Çelebi, H., & Gök, O. (2017). Evaluation of lead adsorption kinetics and isotherms from aqueous solution using natural walnut shell. *International Journal of Environmental Research 11*, 83-90. https://doi.org/10.1007/s41742-017-0009-3

Chu, Y., Khan, M. A., Wang, F., Xia, M., Lei, W., & Zhu, S. (2019). Kinetics and equilibrium isotherms of adsorption of Pb(II) and Cu(II) onto raw and arginine-modified montmorillonite. *Advanced Powder Technology 30*, 1067-1078. https://doi.org/10.1016/j.apt.2019.03.002

Cruz, J. F., Cruz, G. J. F., Ainassaari, K., Gómez, M. M., Solís, J. L., & Keiski, R. L. (2018). Microporous activation carbon made of sawdust from two forestry species for adsorption of methylene blue and heavy metals in aqueous system-case of real polluted water. *Revista Mexicana de Ingeniería Química 17*, 847-861. https://doi.org/10.24275/uam/izt/dcbi/revmexingquim/2018v17n3/Cruz

Doke, K. M., & Khan, E. M. (2017). Equilibrium, kinetic and diffusion mechanism of Cr (VI) adsorption onto activated carbon derived from wood apple shell. *Arabian Journal of Chemistry 10,* S252-S260. https://doi.org/10.1016/j.arabjc.2012.07.031

Guiza, S. (2017). Biosorption of heavy metal from aqueous solution using cellulosic waste orange peel. *Ecological Engineering 99*, 134-140. https://doi.org/10.1016/j.ecoleng.2016.11.043

Ibraheem, A. M., Khan, N., & Mazhar, S. M. (2018). Removal of lead from groundwater of Veppanthattai block, Perambalur district, Tamil Nadu, India using sugarcane bagasse as adsorbent. *World News of Natural Sciences 18*, 213-222.

Jena, S., & Sahoo, R. K. (2017). Removal of Pb (II) from aqueous solution using fruits peel as a low-cost adsorbent. *International Journal of Science, Engineering and Technology 5*, 5-13.

Karimi, Y., Marofi, S., & Zare, M. A. (2018). Removal of lead from polluted water using corn silk as a cheap biosorbent. *Journal of Health Research in Community 4*, 35-48.

Kariuki, Z., Kiptoo, J., & Onyancha, D. (2017). Biosorption studies of lead and copper using roger's mushroom biomass 'Lepiota hystrix'. *South African Journal of Chemical Engineering 23*, 62-70. https://doi.org/10.1016/j.sajce.2017.02.001

Lawal, O. S., Ayanda, O. S., Rabiu, O. O., & Adebowale, K. O. (2017). Application of black walnut (*Juglans nigra*) husk for the removal of lead (II) ion from aqueous solution. *Water Science and Technology 75*, 2454-2464. doi: 10.2166/wst.2017.125

Leizou, K. E., Ashraf, M. A., Chowdhury, A. J. K., & Rashid, H. (2018). Adsorption studies of Pb^{2+} and Mn^{2+} ions on low-cost adsorbent: Unripe plantain (*Musa paradisiaca*) peel biomass. *Acta Chemica Malaysia (ACMY) 2*, 11-15. http://doi.org/10.26480/acmy.01.2018.11.15

Ma, H. T., Ho, V. T. T., Pham, N. B., Bach, L. G., & Phan, T. D. (2018). The comparison of surface modification methods of the heavy metals adsorption of activated carbon from rice husk. *Applied Mechanics and Materials 876*, 91-96. doi: 10.4028/www.scientific.net/amm.876.91

Marimón-Bolívar, W., Tejeda-Benítez, L., & Herrera, A. P. (2018). Removal of mercury (II) from water using magnetic nanoparticles coated with amino organic ligands and yam peel biomass. *Environmental Nanotechnology, Monitoring and Management 10*, 486-493. https://doi.org/10.1016/j.enmm.2018.10.001

Medellín-Castillo, N. A., Hernández-Ramírez, M. G., Salazar-Rábago, J. J., Labrada-Delgado, G. J., & Aragón-Piña, A. (2017). Bioadsorción de plomo (II) presente en solución acuosa sobre residuos de fibras naturales procedentes de la industria ixtlera (*Agave lechuguilla* Torr) y *Yucca carnerosana* (Trel.) McKelvey). *Revista Internacional de Contaminación Ambiental 33*, 269-280.

Mohammad-Rezaei, R. and M. Jaymand, 2019. Graphene quantum dots coated on quartz sand as efficient and low-cost adsorbent for removal of Hg^{2+} and Pb^{2+} from aqueous solutions. *Environmental Progress & Sustainable Energy 38*, S24-S31. https://doi.org/10.1002/ep.12911

Morosanu, I., Teodosiu, C., Paduraru, C., Ibanescu, D., & Tofan, L. (2017). Biosorption of lead ions from aqueous effluents by rapeseed biomass. *New Biotechnology 39*, 110-124. doi:10.1016/j.nbt.2016.08.002

Nikolic, M., Robert, R. J., & Girish, C. R. (2019). The adsorption of cadmium, nickel, zinc, copper and lead from wastewater using tea fiber waste. *Journal of Engineering and Applied Sciences 14*, 7272-7284. 10.36478/jeasci.2019.7743.7755

Naskar, A., & Bera, D. (2018). Mechanistic exploration of Ni (II) removal by immobilized bacterial biomass and interactive influence of coexisting surfactants. *Environmental Progress & Sustainable Energy 37*, 342-354. https://doi.org/10.1002/ep.12685

Obike, A. I., Igwe, J. C., Emeruwa, C. N., & Uwakwe, K. J. (2018). Equilibrium and kinetic studies of Cu (II), Cd (II), Pb (II) and Fe (II) adsorption from aqueous solution using cocoa (*Theobroma cacao*) pod husk. *Journal of Applied Sciences and Environmental Management 22*, 182-190. http://dx.doi.org/10.4314/jasem.v22i2.5

Pollack Velásquez, M., Helfgott Lerner, S., & Tejada Soraluz, J. (2018). El cultivo de caña de azúcar en la costa del Perú durante los eventos de el niño 1982-83 y 1997-98. *Ecología Aplicada 17*, 77-84. http://dx.doi.org/10.21704/rea.v17i1.1176

Ray, J., S. Jana, S.K. Bhanja & T. Tripathy, 2018. Efficient removal f Co (II), Ni (II) and Zn (II) metal ions from binary and ternary solutions using a pH responsive bifunctional graft copolymer. *Colloid and Polymer Science 296*, 1275-1291. 10.1007/s00396-018-4345-4

Sahmoune, M. N. (2019). Evaluation of thermodynamic parameters for adsorption of heavy metals by green adsorbents. *Environmental Chemistry Letters 17*, 697-704. https://doi.org/10.1007/s10311-018-00819-z

Singh, N., Kumari, A., & Balomajumder, C. (2018). Modeling studies on mono and binary component biosorption of phenol and cyanide from aqueous solution onto activated carbon derived from saw dust. *Saudi Journal of Biological Sciences 25*, 1454-1467. https://doi.org/10.1016/j.sjbs.2016.01.007

Tejada-Tovar, C., Gonzalez-Delgado, A. D., & Villabona-Ortiz, A. (2019). Characterization of residual biomasses and its application for the removal of lead ions from aqueous solution. *Applied Sciences 9*, 4486.

Tejada-Tovar, C., Bonilla-Mancilla, D. H., Del Pino-Moreyra, Y., Villabona-Ortíz-A., Acevedo, D. (2018). Removal of Lead (II) of waters from Anticona Cerro de Pasco River (Perú) through the use of orange mesocarpactivated carbon (*Citrus sinensis*). *International Journal of Engineering and Technology (IJET) 10*, 186-196. https://doi.org/10.21817/ijet/2018/v10i1/181001059

Tejada Tovar, C., Herrera, A., & Núñez Zarur, J. (2016). Remoción de plomo por biomasas residuales de cáscara de naranja (*Citrus sinensis*) y zuro de maíz (*Zea mays*). *Revista U.D.C.A.: Actualidad & Divulgación Científica 19*, 169-178. https://doi.org/10.31910/rudca.v19.n1.2016.126

Tejada-Tovar, C., Villabona-Ortiz, Á., & Garcés-Jaraba, L. (2015a). Adsorción de metales pesados en aguas residuales usando materiales de origen biológico. *Tecnológicas 18*, 109-123. https://doi.org/10.22430/22565337.209

Tejada Tovar, C., Villabona Ortiz, Á., & Garcés Jaraba, L. E. (2015b). Kinetics of adsorption in mercury removal using cassava (*Manhiot esculenta*) and lemon (*Citrus limonum*) wastes modified with citric acid. *Ingeniería y Universidad 19*, 283-298. https://doi.org/10.11144/Javeriana.iyu19-2.kamr

Torres-Santillan, E., Capula-Colindres, S., Reza-San German, C. M., Cayetano-Castro, N., & Villagarcia-Chavez, E. (2018). Effect of functional groups in the structure of carbon nanotubes to adsortion grade of cadmium ions. *Revista Mexicana de Ingeniería Química 17*, 955-961. https://doi.org/10.24275/uam/izt/dcbi/revmexingquim/2018v17n3/Torres

US-EPA (2014). Code of Federal Regulations 40 EPA Part 423 Appendix A. US EPA. [Online]:

https://www3.epa.gov/region1/npdes/permits/generic/prioritypollutants.pdf

Verma, S.P. and B. Sarkar. (2018). Simultaneous removal of Cd (II) and p-cresol from wastewater by micellar-enhanced ultrafiltration using rhamnolipid: Flux decline, adsorption kinetics and isotherm studies. *Journal of Environmental Management 213*, 217-235. 10.1016/j.jenvman.2018.02.069.

Vilardi, G., Di Palma, L., & Verdone, N. (2018). Heavy metals adsorption by banana peels micro-powder: Equilibrium modeling by non-linear models. *Chinese Journal of Chemical Engineering 26*, 455-464. https://doi.org/10.1016/j.cjche.2017.06.026

Villabona-Ortíz, A., Tejada-Tovar, C. N., & Ortega-Toro, R. (2020). Modelling of the adsorption kinetics of chromium (VI) using waste biomaterials. *Revista Mexicana de Ingeniería Química 19*, 401-408. https://doi.org/10.24275/rmiq/IA650

Vizcaíno-Mendoza, L., Fuentes-Molina, N., González-Fragozo, H. (2017). Adsorción de plomo (II) en solución acuosa con tallos y hojas de *Eichhornia crassipes*. *Revista U.D.C.A. Actualidad & Divulgación Científica 20*, 435-444. https://doi.org/10.31910/rudca.v20.n2.2017.400

Zhou, Z., Y.G. Liu, S.B. Liu, H.Y. Liu and G.M. Zeng *et al*., 2017. Sorption performance and mechanisms of arsenic (V) removal by magnetic gelatin-modified biochar. *Chemical Engineering Journal 314*, 223-231.https://doi.org/10.1016/j.cej.2016.12.113